Applied Thermal Engineering 114 (2017) 1053–1063

Contents lists available at ScienceDirect

Applied Thermal Engineering

journal homepage: www.elsevier.com/locate/apthermeng

Research Paper

Micro-explosion and burning characteristics of a single droplet of pyrolytic oil from castor seeds

Guan-Bang Chen [a,*], Yueh-Heng Li [a,b], Ching-Hsien Lan [b], Hsien-Tsung Lin [b], Yei-Chin Chao [a,b,*]

[a] Research Center for Energy Technology and Strategy, National Cheng Kung University, Tainan 701, Taiwan, ROC
[b] Department of Aeronautics and Astronautics, National Cheng Kung University, Tainan 701, Taiwan, ROC

HIGHLIGHTS

- Castor pyrolytic oil exhibits a smaller micro-explosion than that of emulsion fuel.
- The residue after combustion is only 0.18% of the weight of the pyrolytic oil.
- Three different stages of micro-explosion are identified.
- During the combustion process, the variation of droplet diameter follows d^2-law.

ARTICLE INFO

Article history:
Received 9 July 2016
Revised 6 December 2016
Accepted 11 December 2016
Available online 16 December 2016

Keywords:
Castor seed
Thermal pyrolysis
Pyrolytic castor oil
Micro-explosion
Droplet combustion
Suspended droplet experiment

ABSTRACT

In the study, castor pyrolytic oil is produced from castor seeds by thermal pyrolysis and its pyrolysis reaction and oxidation reactions are investigated using thermogravimetric analysis. The results are also used to evaluate the characteristic combustion properties, such as the ignition temperature, burnout temperature and combustion characteristics index. The suspended droplet experimental system is also used to explore the micro-explosion phenomena and combustion modes of castor pyrolytic oil under different ambient temperatures. The castor pyrolytic oil is a multi-component fuel and has a complex process during the heating process and micro-explosion occurs, causing the droplet surface distortion. According to the timing and strength of the micro-explosion, there are three different stages: low intensity micro-explosion in the first stage, high intensity micro-explosion in the second stage and medium intensity micro-explosion in the final stage. After high-intensity micro-explosion occurred at 550 °C, more volatile vapors were released and the flammable mixture will formed a flame wrapping around droplets after ignition. During the droplet combustion process, the micro-explosion occurred continuously, but the droplet still maintained a sphere-like appearance. The variation of droplet size generally followed d^2-law and the combustion rate constant is approximately 1.483 mm^2/s.

1. Introduction

Under the emerging threats of drastic climate changing and global warming, carbon-neutral renewable energy is generally considered as a feasible clean alternative energy to partially replace fossil fuel. Renewable energy sources are inexhaustible and make less pollution. Among the various kinds of renewable energy, biomass energy is the most promising, due to its advantages such as biodegradable, less carbon footprint, rich sources, and lower technical threshold. Second only to conventional fossil fuels of coal, oil and natural gas, biomass energy is ranked fourth in the world's total energy consumption [1]. There are plentiful of raw materials that can be converted to biomass energy and among these castor has attracted much attention due to its superior characteristics such as vitality, ability to grow in barren land, as well as being a deep rooted crop and fairly resistant to drought [2].

In general, there are two routes often used for pretreatment processes of biomass conversion, one is biochemical conversion, and the other is thermochemical conversion. Biochemical conversion method refers to the transformation of biomass into fuels, such as biogas or bioethanol using bacteria, microorganisms or enzymes. There are two subcategories for biochemical conversion: digestion (anaerobic and aerobic) and fermentation. In anaerobic digestion, the biomass is converted into methane, carbon dioxide and solid residue. In aerobic digestion, the biomass is converted

* Corresponding authors at: Department of Aeronautics and Astronautics, National Cheng Kung University, Tainan 701, Taiwan, ROC (Y.-C. Chao).
E-mail addresses: gbchen26@gmail.com (G.-B. Chen), ycchao@mail.ncku.edu.tw (Y.-C. Chao).

http://dx.doi.org/10.1016/j.applthermaleng.2016.12.052
1359-4311/

to produce heat, carbon dioxide and solid residue in the presence of oxygen. As to fermentation, the biomass is converted into sugars and the sugar is then converted into bioethanol or other chemicals [3]. Biochemical conversion process does not require much external energy but it is much slower than thermochemical conversion process. Thermochemical conversion refers to degradation of biomass at high temperature and it can be further divided into direct combustion, gasification, pyrolysis and liquefaction [4], and the resulting products can be directly used as fuels, specialty chemicals or electricity precursors. Thermochemical conversion has many outstanding advantages such as, fast reaction, less land requirement, better nutrient replenishment, hazardous pollutants abatement, versatile in input feedstocks, heat removal of active compounds or pathogens, etc. [5].

Castor seeds, which has approximately 50% castor oil, are one of the oil crops which can be used to produce biofuels in the world [6]. After squeezing out the castor seeds, the remaining residue is called castor meal. Nevertheless, because mechanical limitation in the squeezing process, castor meal still contains appreciable amount of castor oil. Chen et al. [7] investigated effects of different parameters on the yield of pyrolytic oil from castor meal. They showed that the maximum yield of 19.61% (g-pyrolytic oil/g-castor meal) pyrolytic oil can be achieved from castor meal. For biomass, thermal pyrolysis is the most promising and simple method to produce liquid products. Pyrolysis typically operates under the condition of absence or lacking of oxygen and the pyrolytic temperature is usually between 300 °C and 750 °C. Many other studies use thermal pyrolysis to obtain bio liquid from various feedstocks such as woody biomass [8], bagasse [9], straw [10], miscanthus [11], oil palm fiber [12], and municipal solid waste [13,4].

Castor seeds contain abundant oil, accounting for approximate 50–60% of the total weight of the seeds. The main components of castor oil include approximately 80.5% ricinoleic acid, 4.2% linoleic acid, 3% oleic acid, 1% palmitic acid, 1% stearyl acid, 0.7% dihydrocarbyl stearate and the other [14]. Castor oil is colorless or pale yellow in color and it has the properties of high viscosity, high density and difficult oxidation. Therefore, it is hardly rancid in air and has good stability for storage. It is a typical non-volatile oil [15]. Castor oil is not frozen until −18 °C and it still retains liquidity at −22 °C after refining. Castor oil can withstand high temperatures of around 600 °C [16], and therefore it is an ideal lubricant for aircraft and industrial machinery [17]. Besides, it can also be used in the production of glycerin, paints, inks, textiles emulsifier, rubber, plastics, biodiesel and other applications. Some ingredients of castor oil can be extracted and refined to use as anticancer drugs, laxatives and drug carriers [18].

In many combustion applications, the liquid fuel is frequently first atomized or pulverized, and then is sprayed or dispersed into the combustion chamber for the purpose of enhancing the evaporation rate. However, the spray combustion is a complex phenomenon of group combustion of droplets. In order to comprehend the behavior of the entire spray, first one has to investigate the heat, mass and momentum transfers leading to ignition and combustion of single droplet in the gas phase medium. For single droplet ignition and combustion, Spalding in 1953 [19] has first proposed and experimentally proved the d^2-law and provided a significant contribution in the droplet evaporation and combustion model.

During the heating process of multi-component droplets, the droplet may swell and suddenly rupture into smaller droplets. This phenomenon was first discovered by Ivanov and Nefedov [20] and was named micro-explosion. During the heating process of a multi-component droplet, the components with low-boiling points first volatilize and the boiling point of the droplet is dominated by the components with high-boiling points. The inside components with low-boiling points are superheated. When they exceed the superheat limit, nucleation occurs and the droplet vaporizes, resulting in the accumulation of internal pressure leading to droplet rupture. Nucleation is a prerequisite for micro-explosion. Nucleation is the beginning stage of the thermodynamic phase change and gaseous bubble generation in the droplet is also a nucleation phenomenon. Nucleation can be divided into homogeneous nucleation and heterogeneous nucleation. When internal low-boiling components within a droplet is superheated to generate bubbles, the bubble generation is the result of homogeneous nucleation. When the nucleation occurs due to impurity or small bubbles, inside the droplet, it is called heterogeneous nucleation.

Micro-explosion can not only accelerate the droplet evaporation in the spray combustion but also provides a convenient strategy for the design of spray combustion systems, that is, micro-explosion makes original large droplets which penetrate deep into the combustion chamber rupture into smaller droplets to achieve the rapid evaporation, ignition and combustion requirement at the proper location of the combustor. Therefore, micro-explosion provides a viable method of improving fuel efficiency. This important micro-explosion process has been the subject of intensive research, especially for miscible multicomponent and water/oil emulsion droplets [21], liquid fuels emulsified with water [22], biodiesel [23] and pyrolytic oil from bio-fuel [24,25]. The micro-explosion process is also shown to be a random process [26] and they the distribution function of the time for the onset of micro-explosion can be correlated with the Weibull distribution.

Pyrolytic oil from castor seeds can be used as a feasible clean alternative energy to partially replace fossil fuel without endangering the food demand of the world. However, above literature survey shows that research concerning the evaporation and combustion characteristics of castor pyrolytic oil is very scarce. Moreover, intensive researches of the characteristic micro-explosion and complex ignition and combustion processes of the castor pyrolytic oil due to the abundant multi-components contained in the pyrolytic oil are worthwhile and warranted. Therefore, in this study, the pyrolysis and the oxidation reaction of castor pyrolytic oil are first studied by thermogravimetric analysis in conjunction with the suspended droplet experiments for the characteristic evaporation behavior, micro-explosion mode, ignition temperature and combustion phenomenon for castor pyrolytic oil droplets.

2. Materials and experimental methods

2.1. Experimental setup

Castor seeds used in this study are provided by the Asian green energy company. Castor seeds are oval-shaped and composed of two parts: the kernel and the shell. The kernel accounts for approximately 70–75% of the total weight of a seed and is rich in oil, which is called castor oil. The experimental apparatus for thermal pyrolysis is shown in Fig. 1. In this study, at first, 100 g of castor seeds was packed in a cylindrical container with the diameter of 32 mm and the length of 240 mm. The material of the feedstock container was stainless steel 316 and it can resist pitting and crevice corrosion. Therefore, there was no chemical reactions occurred between the container and the pyrolytic product during the pyrolysis process. The container was put into a quartz tube, which is placed in the tube furnace. The quartz tube was vacuumed by a vacuum pump (MZ 2C, Vacuubrand), and then filled with nitrogen to ambient pressure. The pyrolytic temperature was 400 °C with a heating rate of 20 °C/min, and then maintained at this temperature for 60 min. These operation conditions are based on our previous study for the maximum yield of castor pyrolytic oil [7]. The released volatile gas flowed to a condensing system to produce

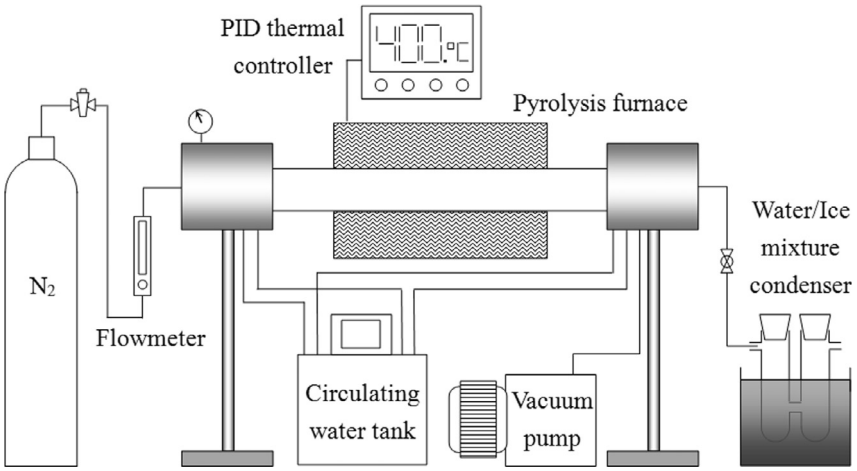

Fig. 1. The experimental setup for thermal pyrolysis.

the bio liquid. The pyrolytic liquid was placed for 24 h and then was divided into pyrolytic oil and aqueous product using a separatory funnel. The remaining uncondensed gas was discharged through the exhaust system. The residues in the container was castor biochar after the furnace was cooled to room temperature. The average pyrolytic liquid is about 53% of the total weight of a seed, which can be divided into 42% pyrolytic oil and 11% aqueous product.

2.2. Thermogravimetric analysis (TGA)

In the study, thermal analysis (TA Instruments, SDT Q600) was used to simultaneously implement TGA and differential scanning calorimetry (DSC). Details of the thermal analysis system and methods of thermogravimetric analysis employed in this study can be found in a previous article by our group [7]. The thermal analysis was carried out at the temperature range of 30 °C and 1200 °C, and the corresponding heating rate was 10 °C/min. The testing sample of 8 mg was placed in a 90 μL platinum crucible, and the flow rate of carrying gas (nitrogen or air) was set to 50 mL/min.

2.3. Suspended droplet experimental system

The suspended drop method is commonly used in the study of single droplet ignition and combustion [23–25]. The single droplet is capillarily suspended by a quartz fiber or a thermocouple, whereby the evaporation or combustion characteristics of the droplet during the heating process can be observed.

The experimental setup for the suspended droplet in the study is shown in Fig. 2. The heating device consists of two ceramic heating plates with a separation distance of 9 mm and the size of each side ceramic heating plate is 60 mm. This ceramic heating plate is a nickel-chromium alloy heating wire wound around the ceramic sheet (aluminum oxide doped with magnesium oxide). An 110 V/400 W power supply and the programmable temperature controller (Shinko Technos: PCD-33A) are used to control the output power. In this study, the heating device can provide a surrounding temperature of the suspended droplet up to 600 °C, which is measured by a K-type thermocouple. The experiments were started when the heating plates were heated to attain the target temperature of the surrounding temperature of the suspended droplet (350 °C, 450 °C and 550 °C) and became stable.

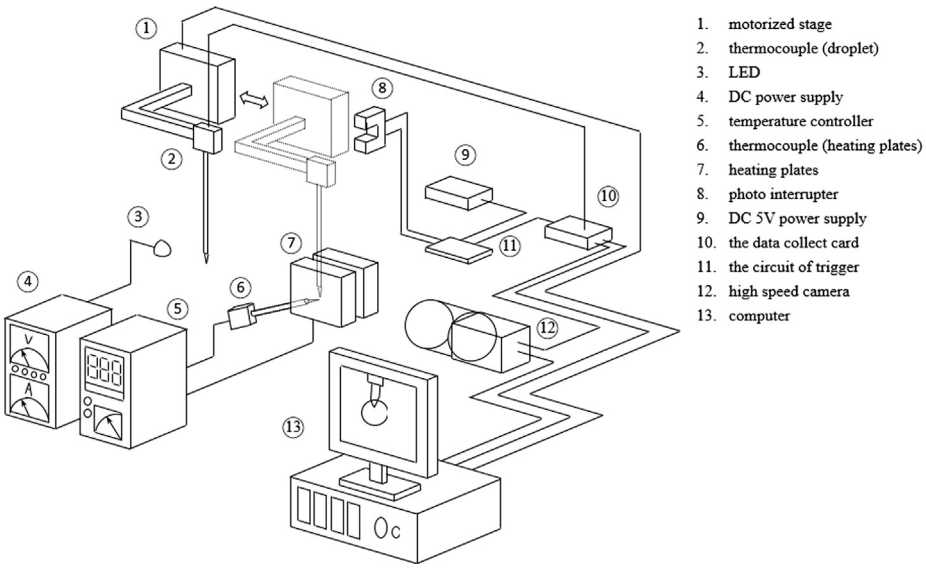

Fig. 2. The schematic of the experiment apparatus for suspended drop.

The experiment was conducted by placing a single droplet of castor pyrolytic oil on the junction of a K-type thermocouple which measured the temperature of the oil drop during the experiment and another thermocouple was also used with a temperature controller to control the environment temperature between the heating plates. After a single droplet was suspended on the thermocouple, it was rapidly transported to the heating plates by a motorized stage (Zaber: T-LSM100A-KT03). The maximum moving speed of the stage is 7 mm/s and the accuracy is 1 μm. The stage can move the droplet to exactly the same position of the thermal field for all the experiments. When the thermocouple was in the preset position, the motorized stage would touch the switch, and simultaneously triggered the high speed camera (Cooke: PCO.1200hs) and the data acquisition system (DAQ, National Instrument: BNC-2110) for image and signal recording.

2.4. The combustion characteristic parameters

Several combustion characteristic parameters which are often used to evaluate the bio-fuels can be deduced from a thermogravimetric/derivative thermogravimetric (TG-DTG) curves. In this study, the characteristic combustion parameters of ignition temperature (T_i), burnout temperature (T_e), and combustion characteristics index (S) for castor pyrolytic oil will be used and compared with those of heavy fuel oil to characterize its combustion properties. There are many methods to identify the ignition temperature using TG-DTG curves [27–29], and the method proposed by Tognotti et al. [27] is widely used to predict the ignition temperature for different fuels. In their method, the TG curve in the air atmosphere initially will overlap with that in the N_2 atmosphere, and the ignition temperature (T_i) is defined to be the temperature corresponding to the first bifurcation point in these two curves. The burnout temperature (T_e) is often defined as the temperature corresponding to 99% mass conversion ratio of the burnable part of the fuel in the air atmosphere [30–32].

The ignition and burnout temperatures show only specific combustion property of the fuel, therefore integrated indices are often useful to globally evaluate combustion performance of the fuel. The combustion characteristic index (S) is often used for benchmarking the combustibility of fuels [33] and it was first proposed by Cheng et al. [34]. The larger the combustion characteristics index, the better the combustion characteristics of the fuel. The combustion rate is expressed by the Arrhenius equation, as follows:

$$dW/d\tau = A\exp(-E/RT) \quad (1)$$

where W is the conversion ratio, τ is the time, $dW/d\tau$ is the combustion rate, A is a pre-exponential factor, E is the activation energy, R is the ideal gas constant and T is the absolute temperature.

Take the differential of Eq. (1) with temperature and rearrange it as follows,

$$\frac{R}{E}\times\frac{d}{dT}\left(\frac{dW}{d\tau}\right)=\frac{dW}{d\tau}\times\frac{1}{T^2} \quad (2)$$

At ignition temperature T_i, Eq. (2) is multiplied by $\frac{(dW/d\tau)_{max}(dW/d\tau)_{mean}}{(dW/d\tau)_{T=T_i}T_e}$:

$$\frac{R}{E}\times\frac{d}{dT}\left(\frac{dW}{d\tau}\right)_{T=Ti}\frac{(dW/d\tau)_{max}}{(dW/d\tau)_{T=Ti}}\times\frac{(dW/d\tau)_{mean}}{T_e}=\frac{(dW/d\tau)_{max}\times(dW/d\tau)_{mean}}{T_i^2\times T_e} \quad (3)$$

where $(dW/d\tau)_{max}$ is the maximum combustion rate, which can be obtained from the peak of DTG curve. $(dW/d\tau)_{mean}$ is the mean combustion rate, which can be obtained from the mean of DTG curve. The first term of Eq. (3) on the left hand side represents the reaction strength of fuel combustion which is related to the fuel. The second term stands for the change rate of fuel combustion rate at the ignition temperature and the third term refers to the ratio of maximum combustion rate to the combustion rate at the ignition temperature. These two terms are related to the ignition tempera-

Table 2
Ultimate analysis of diesel, heavy fuel oil, and castor pyrolytic oil.

Fuel	N (%)	C (%)	H (%)	O (%)	S (%)
Diesel	–	84.75	12.46	–	0.22
Heavy fuel oil	0.00	86.91	11.56	0.73	0.46
Castor oil (pyrolytic)	3.11	71.65	10.52	13.52	0.00

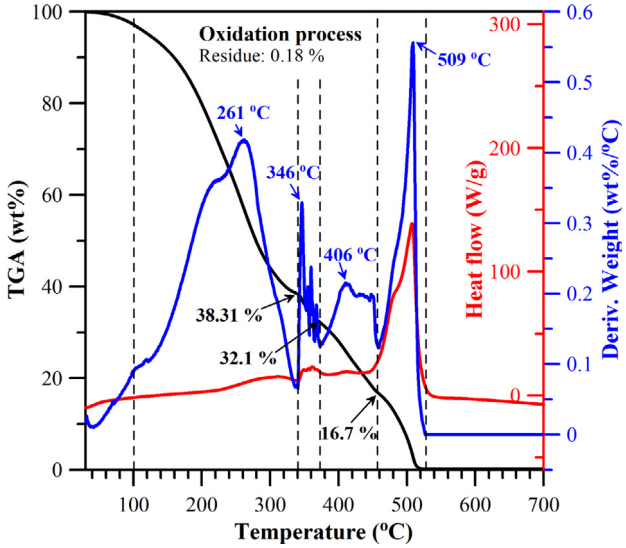

Fig. 3. TGA burning profile of pyrolytic oil obtained from castor seed (air flow rate: 50 mL/min, heating rate: 10 °C/min).

Table 3
The combustion characteristic parameters of different fuels.

Fuel	$(\frac{dW}{d\tau})_{max}$	$(\frac{dW}{d\tau})_{mean}$	T_i (°C)	T_e (°C)	S ×10^7
Castor pyrolytic oil	5.520	1.991	328	513	1.997
Sludge pyrolytic oil	4.360	1.162	274	605	1.114
Heavy fuel oil	3.517	1.544	434	612	0.470

Table 1
Properties of different kinds of fuel oil.

Properties	Diesel	Heavy fuel oil	Castor oil (pyrolytic)	Test method
Density (kg/m^3, @15 °C)	0.8335	0.9533	0.966	ASTM D4052
Viscosity (CST, @40 °C)	3.024	130.3	81.47	ASTM D445
Flash point (°C)	52–80	110	37	ASTM D93
Pour point (°C)	−9	12	−6	ASTM D97
Heating value (MJ/kg)	42.496	44.877	34.775	ASTM D240
Water content (vol%)	–	0.32	2.5	ASTM E203

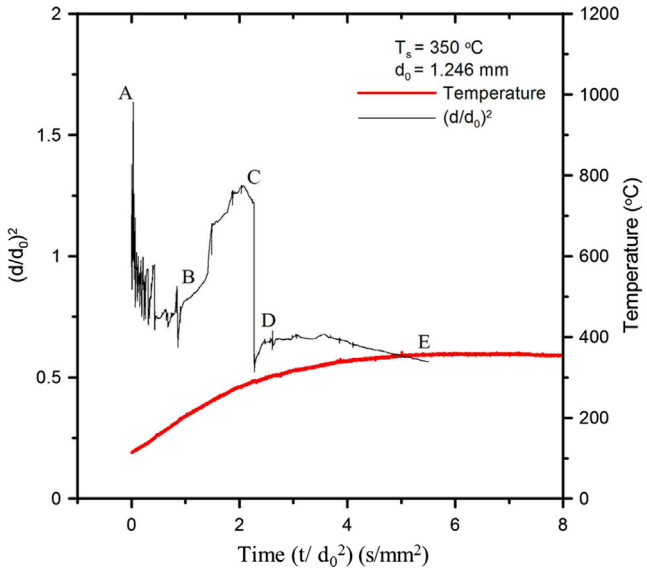

Fig. 4. The variation of droplet size $(d/d_0)^2$ and characteristic time (t/d_0^2) with time at an ambient temperature of 350 °C. d_0 is the initial droplet diameter and d is the droplet diameter at time t.

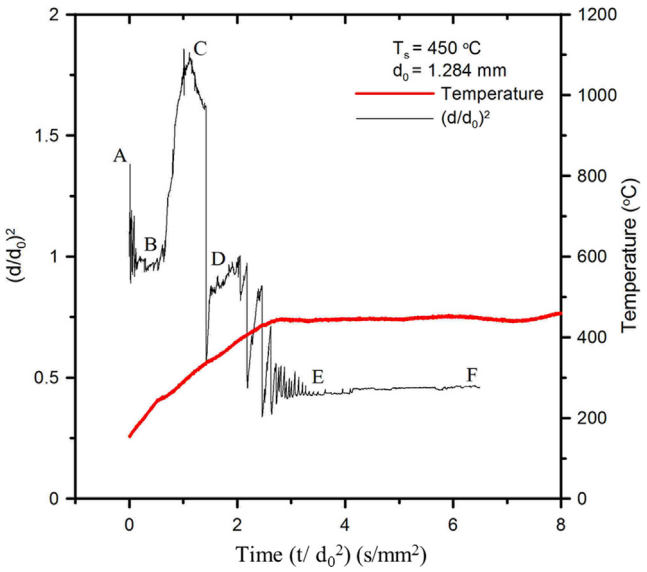

Fig. 6. The variation of droplet size $(d/d_0)^2$ and characteristic time (t/d_0^2) with time at an ambient temperature of 450 °C. d_0 is the initial droplet diameter and d is the droplet diameter at time t.

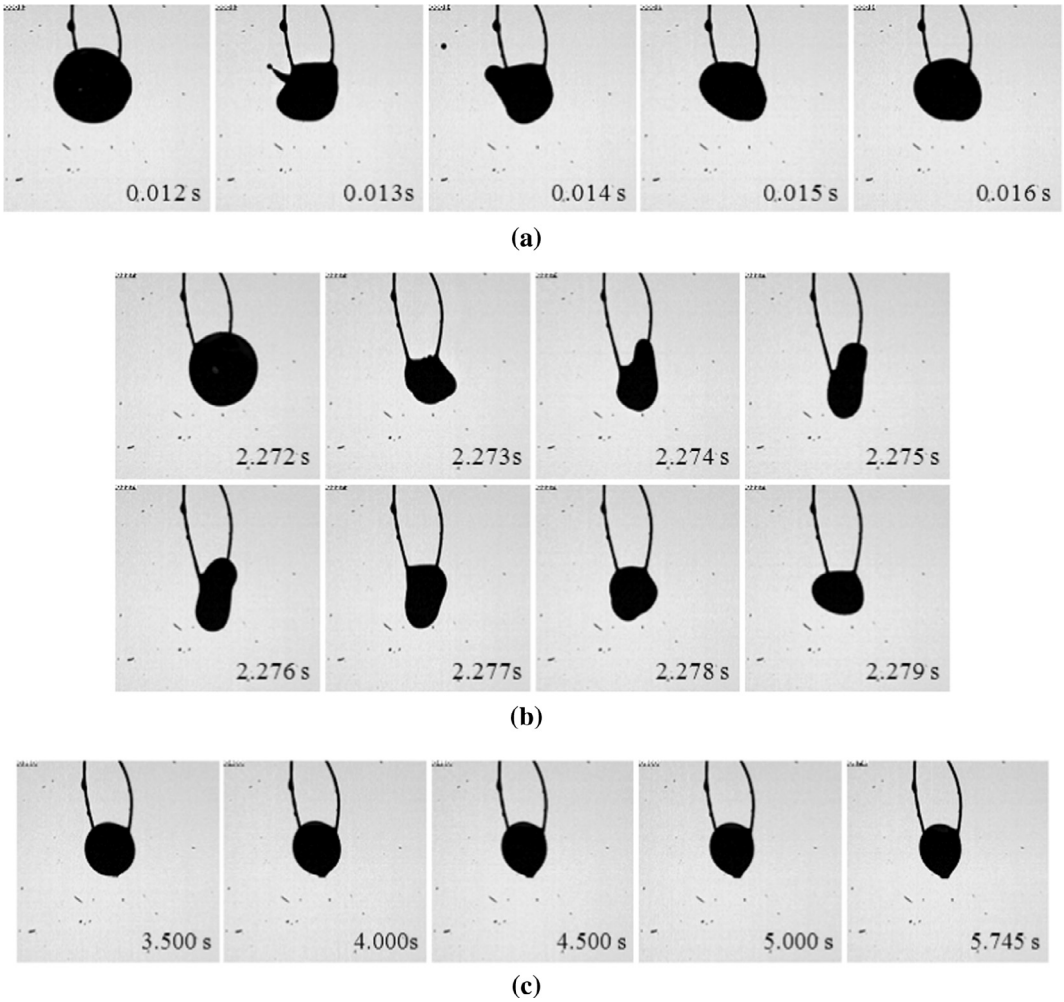

Fig. 5. Heating processes of a droplet at an ambient temperature of 350 °C (a) the first stage, (b) the second stage, (c) the third stage.

ture. The last term is the ratio of mean combustion rate to the burnout temperature and the larger the value, the shorter the burnout time of the fuel. Finally, the right hand side of Eq. (3) is the combustion characteristic index (S):

$$S = \frac{(dW/d\tau)_{max} \times (dW/d\tau)_{mean}}{T_i^2 \times T_e} \quad (4)$$

3. Results and discussion

3.1. Properties of castor pyrolitic oil

Table 1 shows the physicochemical properties of diesel, heavy fuel oil, and castor pyrolytic oil for comparison. The test methods are also shown in Table 1. The viscosity of castor pyrolytic oil is

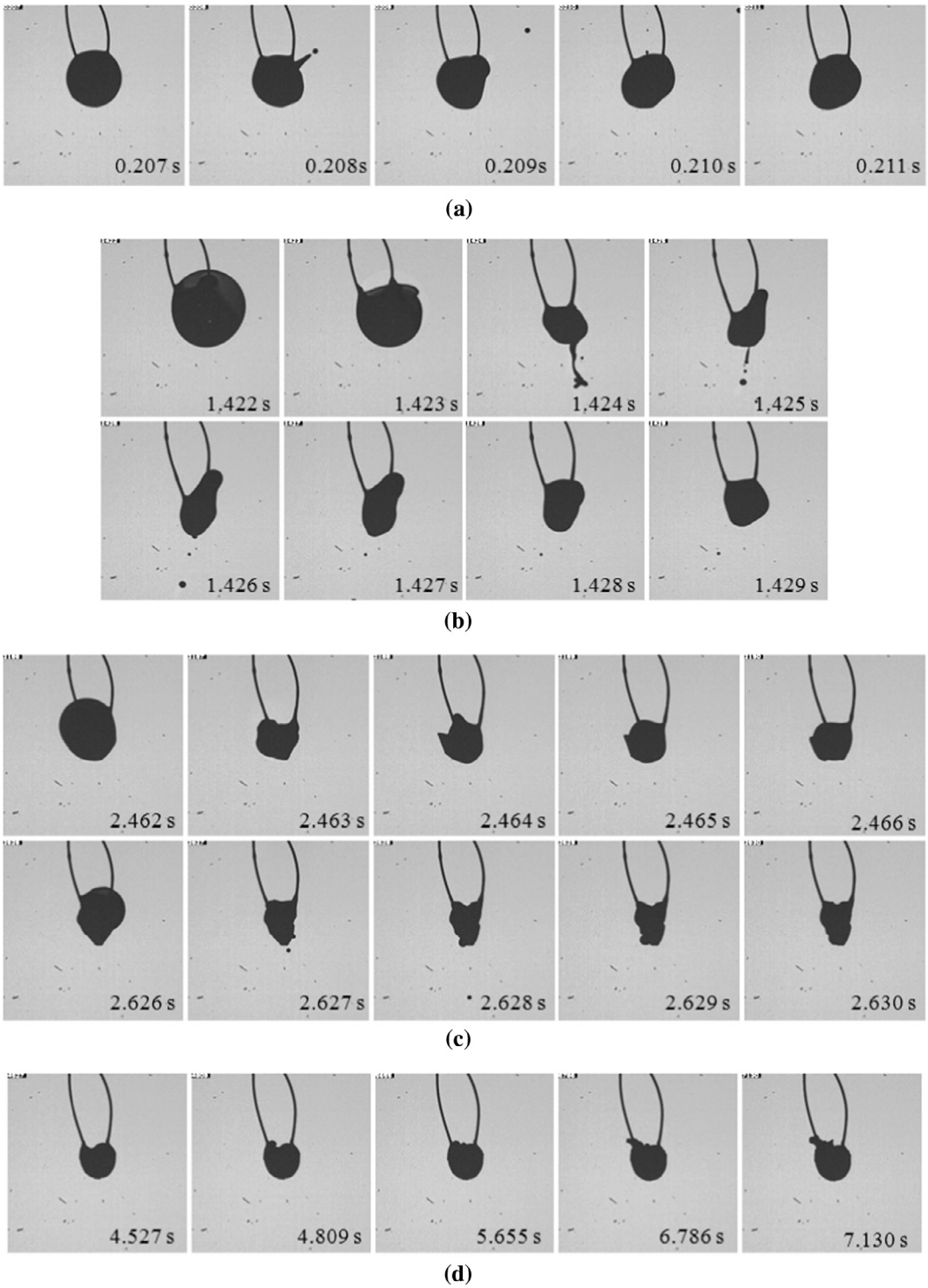

Fig. 7. Heating processes of a droplet at an ambient temperature of 450 °C (a) the first stage, (b) the second stage (first micro-explosion occurs) (c) the second stage (after first micro-explosion) (d) the thrid stage.

between that of diesel and heavy fuel oils. The flash point of castor pyrolytic oil is close to that of diesel. In addition, the pour point of castor pyrolytic oil is also close to that of diesel, which means it still retains the mobility at low temperatures. In terms of heating value, although castor pyrolytic oil has slightly lower heating value than that of diesel or heavy fuel, it is still significantly higher than the common bio-oil from lignocellulose. Castor pyrolytic oil has considerable potential regardless of direct use as a fuel or mixed with diesel fuel, heavy fuel oil or other hydrocarbon fuels. The water content of castor pyrolytic oil used in this study is also detected and it is not more than 2.5%. When compared to some other bio-oils (for example, lauan: 18–27% [35], oak: 16.1% [36], pine: 18.5% [36]), it has a relatively low water content. The ultimate analysis of castor pyrolytic oil is shown in Table 2 and it is shown that the sulfur is not detected. Castor pyrolytic oil has almost negligible sulfur concentration and is almost SO_x pollution-free when burned as fuel.

3.2. Thermogravimetric analysis of castor pyrolytic oil

Singh et al. [37] studied the effects of temperature on the pyrolysis of castor seeds for the maximum liquid yield. They also analyzed major compounds in the castor pyrolytic oil. Fig. 3 shows the thermogravimetric curve of castor pyrolytic oil in air environment. The green curve is TG (thermogravimetry), the blue curve is DTG (differential of TG) and the red curve is DSC (differential scanning calorimetry). In Fig. 3, there are four distinct peaks in the DTG curve. Weight loss primarily occurs in the range of 100–340 °C, 340–373 °C, 373–458 °C and 458–525 °C, and the corresponding maximum rate of weight loss occurs at 261 °C, 346 °C, 406 °C and 509 °C, respectively. In the first stage of the weight loss, the weight loss accounts for 61.69%, and it is due to the decomposition and/or evaporation of components with low boiling points. For example, the boiling temperatures of Octadec-9-enoic acid and 10-Undecenoic acid are close to 171 °C and 275 °C, respectively. The second and third stages of weight loss occur between 340–373 °C and 373–458 °C, respectively and they are attributed to the decomposition and/or evaporation of components with boiling temperatures in the range of about 340 °C and 460 °C. For example, the boiling temperatures of N-hexadecanoic acid, Oleic acid, Octadecanoic acid and 9-Octadecenamide, (Z)- are close to 352 °C, 360 °C, 361 °C and 433 °C, respectively. DSC curve also indicates exothermic reactions in these two stages. In the final stage between 458 and 525 °C, there is a sharp peak in the DSC curve at 509 °C, which represents the occurrence of intense combustion reactions. After the reaction, the residue is only about 0.18% of the original weight of the pyrolytic oil, which displays the characteristics of low ash content of the castor pyrolytic oil. Conceicção et al. [38] investigated thermal and oxidative degradation of castor oil. They also found that TG/DTG curves of castor oil inhibited multistage reactions, attributed to decomposition and/or volatilization of triacylglycerides (mainly ricinoleic acid), in the temperature ranges of 221–395, 395–482, and 482–573 °C, respectively. The DSC curve of castor oil presented exothermic transitions, attributed to the combustion process, in the peak temperatures of 347, 434 and 541 °C, respectively.

The results of thermogravimetric analysis are used to calculate the ignition temperature, burnout temperature and combustion characteristics index (S) of castor pyrolytic oil. Table 3 shows the comparison of the combustion characteristic parameters for castor pyrolytic oil, sludge pyrolytic oil [39] and heavy fuel oil [39]. Among these fuels, sludge pyrolytic oil has the lowest ignition temperature and heavy fuel oil has the highest one, since it has less volatile matter. Castor pyrolytic oil has the lowest burnout temperature in these fuels and the burnout temperatures for sludge pyrolytic oil and heavy fuel oil are very close. Table 3 also shows that the maximum and mean combustion rates of castor pyrolytic oil are highest among these three fuels. Finally, according to Eq. (4), castor pyrolytic oil has the maximum value of the combustion characteristics index, which is used to globally characterize the combustion performance of the fuel. The fuel with a high combustion characteristic index is predominant because the fuel is easy to ignite and has short burnout time and strong reaction strength.

3.3. Thermal behavior of a single droplet

Castor pyrolytic oil is a multi-component fuel and therefore has a wide boiling range. It results in a complex process during the heating process and micro-explosion occurs, causing distortion of the droplet surface. In addition, because of the high viscosity and low water content, the micro-explosion strength of castor pyrolytic oil is smaller than that of emulsion fuels.

Fig. 4 shows the variation of suspended droplet size and temperature of castor pyrolytic oil at the ambient temperature of 350 °C. The ordinate is dimensionless drop size $(d/d_0)^2$ and the abscissa is characteristic time (t/d_0^2). Fig. 5 shows the image sequence of a droplet at ambient temperature of 350 °C for different stages. The results show that micro-explosion phenomena occur and droplet size has a complex change in the heating process. The evolution of droplet size during heating can be divided into three stages:

(1) The surface micro-explosion stage that micro-explosion occurs near the surface of the droplet (A-B in Fig. 4): The compounds with low boiling point near the surface are first heated and evaporated, and nucleation occurs near the droplet surface. It induces persisting micro-explosion with smaller intensity, and causes continuous distortion of the droplet shape (as shown in Fig. 5(a)). This stage ends when the droplet was heated to about 170 °C. During the micro-explosion process of this stage, eruption of small droplets, or simply release of oil vapor with low-boiling point compounds into the external environment are generally found.
(2) The nucleation micro-explosion stage that nucleation occurs in the interior of the droplet leading to droplet swelling and micro-explosion (B-C-D in Fig. 4): When the droplet is further heated to 200 °C, the boiling point is dominated by

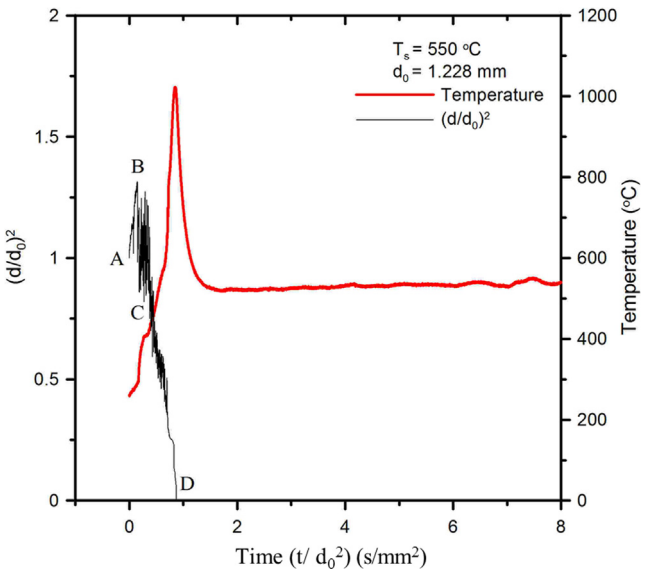

Fig. 8. The variation of droplet size $(d/d_0)^2$ and characteristic time (t/d_0^2) with time at an ambient temperature of 550 °C. d_0 is the initial droplet diameter and d is the droplet diameter at time t.

the compounds with high boiling point. Therefore, the internal low-boiling compound of the droplet would be superheated. After exceeding superheating limit, it starts to form homogeneous nucleation and evaporation occurs. The pressure inside the droplet accumulates, so that the droplet begins to swell and micro-explosion occurs at a temperature of about 300 °C (as shown in Fig. 5(b)). During this stage, the droplet might be pull into smaller droplets or broken into pieces, or simply releasing of the oil vapor into the external environment. In addition, when the droplets are heated to about 260 °C, there will be significant expansion for the droplet instantaneously. According to the results of Singh et al. [37], 10-Undecenoic acid accounts for the largest proportion of castor pyrolytic oil. Its boiling temperature is close to 260 °C. Therefore, we believe that the significant expansion of the droplet at 260 °C is due to the evaporation of 10-Undecenoic acid.

(3) Droplet residue stage (D-E in Fig. 4): it has the residue of castor pyrolytic oil on the thermocouple wire and the size is not obviously changed. The remaining oil is mainly the high-boiling components and it is difficult to valitalize in the environment at temperature of 350 °C (as shown in Fig. 5(c)).

Fig. 6 shows the variation of suspended droplet size and temperature of castor pyrolytic oil at the ambient temperature of 450 °C and Fig. 7 shows the image sequence of a droplet for different stages. Like the case at the ambient temperature of 350 °C, the variation of droplet size can be divided into three stages:

(1) The surface micro-explosion stage (A-B in Fig. 6): The behavior of this stage is similar to the case of 350 °C. Since the compounds with low boiling point near the surface are heated and evaporated, and nucleation occurs near the droplet surface, microexplosion with smaller intensity persists, and the droplet shape is continuously changed (as shown in Fig. 7(a)). This stage ends when the droplet was heated to about 200 °C. During the micro-explosion process, it may have the eruption of small droplets, or simply the oil vapor with low-boiling points released into the external environment.

(2) The nucleation micro-explosion stage (B-C-D-E in Fig. 6): When the droplet is further heated to 260 °C, the boing point is dominated by the compounds with high boiling point. Therefore, the internal low-boiling compound would be superheated. After exceeding superheating limit, homoge-

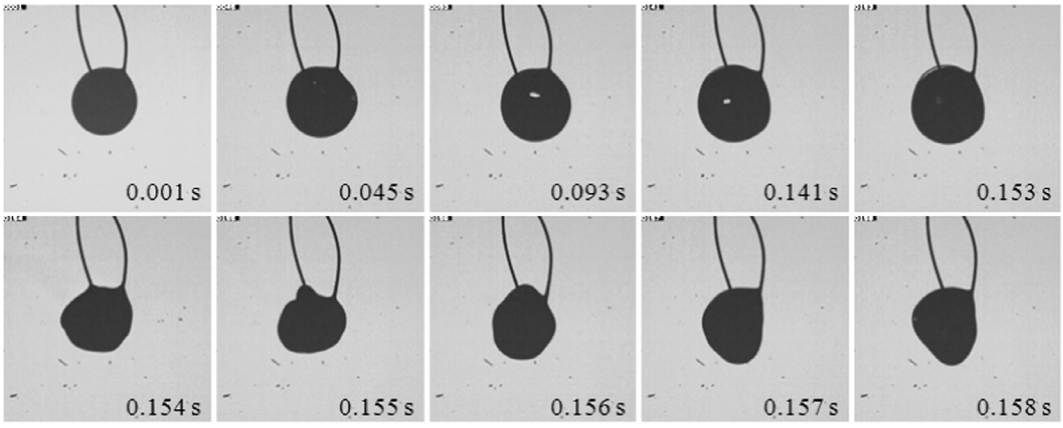

(a)

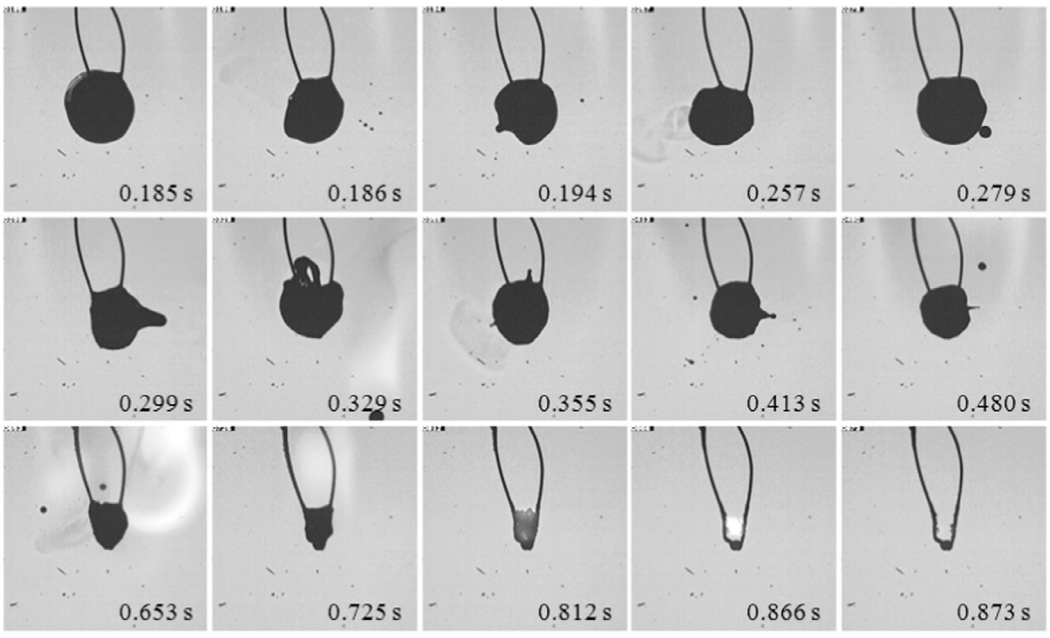

(b)

Fig. 9. Heating processes of a droplet at an ambient temperature of 550 °C (a) the first stage, (b) the second stage.

neous nucleation and evaporation occur. The pressure inside the droplet accumulates, so that the droplet begins to swell and micro-explosion occurs at a temperature of about 340 °C (as shown in Fig. 7(b)). During the micro-explosion process, the droplet might be pull into smaller droplet or broken into pieces and the oil and gas will be released into the external environment. In addition, after high-intensity microexplosion at about 340 °C, microexplosion still persists until about 450 °C as shown in Fig. 7(c). It exists a continuous loop for the droplet with nucleation of internal bubble and breakdown with small droplets eruption, which is similar to the type of high-strength microexplosion at 340 °C. The difference is in the microexplosion strength and the size of erupted droplet are smaller in this process. After this high strength micro-explosion, a series of lower-intensity microexplosion occur. According to the results of Singh et al. [37], N-hexadecanoic acid, Oleic acid and Octadecanoic acid account for 5.55%, 17.89% and 11.92% of castor pyrolytic oil, respectively. Their boiling temperatures are close to 352 °C, 360 °C and 361 °C, respectively. Therefore, we believe that the series of lower-intensity micro-explosion after 350 °C is particularly due to the evaporation of N-hexadecanoic acid, Oleic acid and Octadecanoic acid.

(3) Droplet residue stage (E-F in Fig. 6): When the drop microexplosion ends, the volatile matter of castor pyrolytic oil almost volatiles to the environment and it will eventually have a black residual solid on the thermocouple. In general, there will be no change in size of this black solid. However, in certain situations it may be found that the solid become bigger after a period of time. This phenomenon is not like the droplet expansion and it grows solid material in local position as shown in Fig. 7(d).

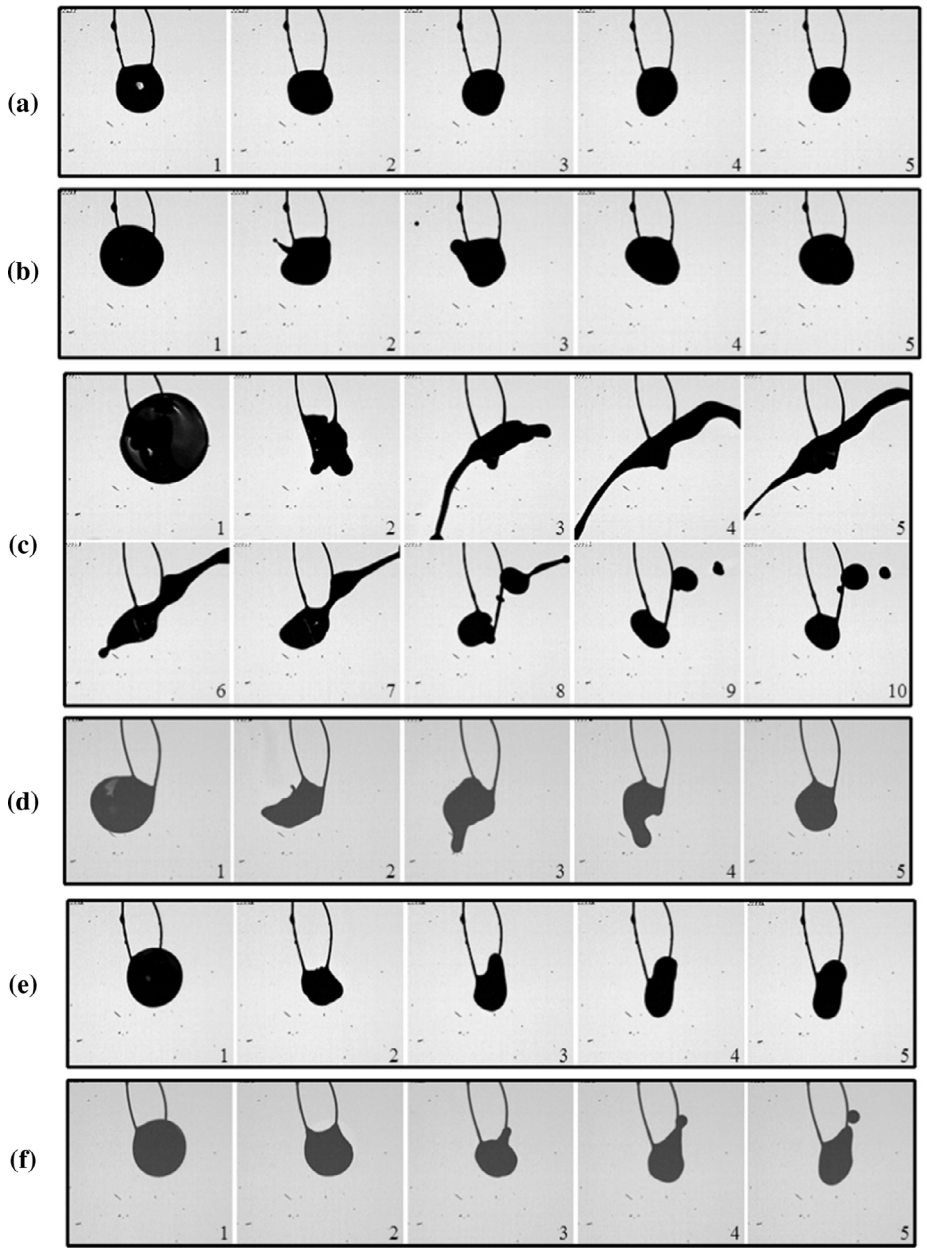

Fig. 10. Different Modes of micro-explosion: (a) Mode 1-a (100–200 °C), (b) Mode 1-b (100–200 °C) (c) Mode 2-a (200–350 °C), (d) Mode 2-b (200–350 °C), (e) Mode 3-a (300–450 °C), (f) Mode 3-b (300–450 °C).

Fig. 8 shows the variation of suspended droplet size and temperature of castor pyrolytic oil at the ambient temperature of 550 °C and Fig. 9 depicts the image sequence of a droplet for different stages. At this high temperature, droplet ignition and combustion can be observed. The variation of droplet size can be divided into two stages:

(1) Droplet swell and burst stage (A-C in Fig. 8): At 550 °C, low boiling components inside the droplet are heated rapidly and volatilization and nucleation occur instantaneously, as shown in Fig. 9(a). The pressure inside the droplet quickly increases, and the droplet begins to swell and burst with a strong micro-explosion at a temperature of about 200 °C, accompanied by a certain amount of oil and gas release from the droplet interior.
(2) Droplet combustion stage (C-D in Fig. 8): Volatile vapor is released in the previous stage and the flammable mixture is ignited to form a non-premixed flame wrapping around the droplet (as shown in Fig. 9(b)). Combustion accelerates the heating rate of the droplet, and micro-explosion continues to occur because of the nucleation of volatile compounds inside the droplet. The droplet shape is dramatically distorted, and the release of oil and gas affect the appearance of the flame. In addition, the small droplets ejected from the main droplet during the micro-explosion process also are ignited, and formed a small flame. In the following droplet combustion stage, volatile components are completely burned, residual solid particle continues to burn, and almost no residue remained.

These results indicate that heating a drop of castor pyrolytic oil engenders several types of micro-explosion. According to the timing and strength of the micro-explosion observed in this study, the micro-explosion occurs in three different modes and each mode can be divided into two types on the basis of the conditions after micro-explosion, as show in Fig. 10. Mode 1 occurs mainly in the initial heating period of droplets (100–200 °C) and involves only the release of volatile substances within the nucleus bubbles after micro-explosion (Fig. 10(a)), or an additional eruption of small droplets (Fig. 10(b)). Mode 2 occurs mainly in the middle heating period of droplets (200–350 °C). After micro-explosion, the droplet is pulled into the liquid column. Subsequently, the liquid column will be broken into small pieces (Fig. 10(c)) or reverted to a sphere (Fig. 10(d)). During the mode 2 micro-explosion process, more volatile substances are released. Mode 3 occurs mainly after Mode 2 (300–450 °C). Similar to mode 1, after the micro-explosion, Mode 3 involves only the release of volatile substances within the nucleus bubbles (Fig. 10(e)) or an additional eruption of small droplets (Fig. 10(f)). The order of the micro-explosion strength is Mode 2 > Mode 3 > Mode 1.

Castor pyrolytic oil can be ignited at the temperature of 550 °C and ignition occurs after the occurrence of Mode 2 micro-explosion because of the release of more volatile vapor. The flammable mixture forms a flame wrapping around droplets after it is ignited in high temperature environments. During the droplet combustion process, the micro-explosion occurs continuously; however, the droplet still maintains the sphere-like appearance. Subsequently, the droplet rapidly evaporates and the flame wraps around the droplet. The droplet size varies with time in the combustion process and this combustion characteristic generally follows the d^2-law. Fig. 11 illustrates a curve fitting of droplet size $(d/d_0)^2$ variation and its slope at ambient temperature of 550 °C. As show in Fig. 11, it can be approximated using a straight line and the slope K, which denotes the combustion rate constant, is approximately 1.483 mm^2/s.

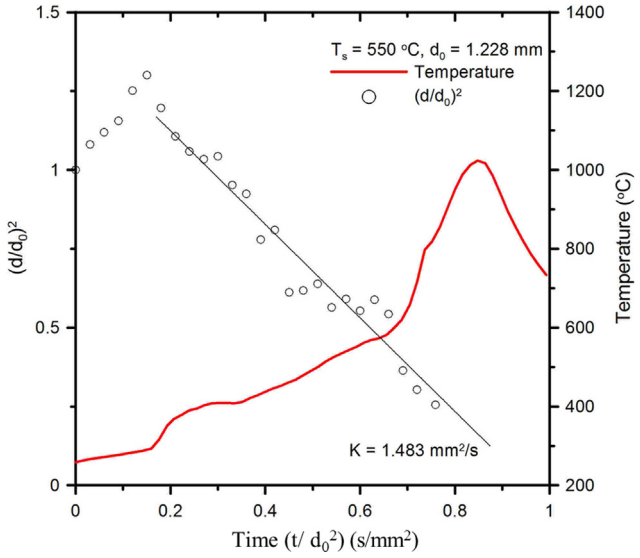

Fig. 11. The curve fitting of droplet size $(d/d_0)^2$ variation and its slope at an ambient temperature of 550 °C. d_0 is the initial droplet diameter and d is the droplet diameter at time t.

In the following stage of the droplet combustion process, volatile components are completely evaporated and residual solid particle continues to burn. According to the temperature measured using the thermocouple, the combustion of solid particles could exceed 1200 °C and almost no residue is observed after burning. This is consistent with the thermogravimetric analysis result, which reveals almost no ash after the burning of castor pyrolytic oil.

In summary, castor pyrolytic oil from castor seeds exhibits a complex micro-explosion behavior, its ignition temperature is lower than that of diesel and heavy fuel oil and its combustion characteristics follow d^2-law. Furthermore, it undergoes almost complete combustion with a negligible amount of residue and thus suitable for use as a fuel.

4. Conclusions

In the study, castor oil was produced through thermal pyrolysis and its oxidation reactions were investigated through thermogravimetric analysis. Moreover, the suspended droplet experimental system was used to explore the micro-explosion phenomenon and combustion modes of castor pyrolytic oil at various ambient temperatures (350 °C, 450 °C and 550 °C). The following findings were obtained.

1. Castor pyrolytic oil is a kind of multicomponent fuel, it has a broad boiling range, which facilitates the occurrence of micro-explosion and causes droplet surface distortion. In addition, because of its high viscosity and low water content, castor pyrolytic oil exhibits a smaller micro-explosion than that of emulsion fuel.
2. Results from thermogravimetric analysis indicate the main oxidation reactions of castor pyrolytic oil occurred between 100 °C and 320 °C. The maximum weight loss occurred between 100 °C and 320 °C. Its non-volatile components may be ignited at approximately 500 °C and the residue was only nearly 0.18% of the original weight of the pyrolytic oil.
3. The combustion characteristic parameters of castor pyrolytic oil such as ignition temperature T_i = 328 °C, burnout temperature T_e = 513 °C, and combustion characteristics index S = 1.991 ($10^{-7}\cdot\%^2\cdot K^{-3}\cdot min^{-2}$) were obtained through thermogravimetric analysis.

4. The pyrolytic oil of castor seeds is a multi-component fuel and therefore has a wide boiling range. It thus undergoes a complex process during heating and micro-explosion occurs, causing droplet surface distortion. According to the timing and strength of the micro-explosion, three stages were identified and are outlined as follows: low intensity micro-explosion in the first stage, high intensity micro-explosion in the second stage and medium intensity micro-explosion in the final stage.
5. After high-intensity micro-explosion occurred at an ambient temperature of 550 °C, more volatile vapor were released and the flammable mixture formed a flame wrapping around droplets after ignition in high temperature environments. During the droplet combustion process, the micro-explosion occurred continuously, but the droplet still maintained a sphere-like appearance. The droplet rapidly evaporated and the flame wrapped the droplet. The fuel combustion characteristics substantially followed d^2-law. The variation of droplet diameter with time can be approximated using a straight line with a constant slope of 1.483 mm^2/s. In the latter stage of the droplet combustion, volatile components were completely evaporated, residual solid particles continued to burn, and almost no residue remained after burning.

Acknowledgements

This research was supported by the National Science Council of the Republic of China under the grant number NSC 101-3113-P-468-001.

References

[1] International Energy Agency, Key World Energy Statistics, IEA Publications, Paris, 2016, p. 6.
[2] Castoroil.in, Online Bookmark of Castor, 2013. From: <http://www.castoroil.in>.
[3] P. Basu, Biomass Gasification, Pyrolysis and Torrefaction: Practical Design and Theory, Academic Press, 2013, ISBN 978-01-239-6543-1.
[4] K.B. Cantrell, T. Ducey, K.S. Ro, P.G. Hunt, Livestock waste-to-bioenergy generation opportunities, Bioresour. Technol. 99 (2008) 7941–7953.
[5] K. Cantrell, K. Ro, D. Mahajan, M. Anjom, P.G. Hunt, Role of thermochemical conversion in livestock waste-to-energy treatments obstacles and opportunities, Ind. Eng. Chem. Res. 46 (2007) 8918–8927.
[6] L. López-Bellido, J. Wery, R.J. López-Bellido, Energy crops: prospects in the context of sustainable agriculture, Eur. J. Agron. 60 (2014) 1–12.
[7] G.L. Chen, G.B. Chen, Y.H. Li, W.T. Wu, A study of thermal pyrolysis for castor meal using Taguchi method, Energy 71 (2014) 62–70.
[8] S. Karagoz, T. Bhaskar, A. Muto, Y. Sakata, T. Oshiki, T. Kishimoto, Low-temperature catalytic hydrothermal treatment of wood biomass: analysis of liquid products, Chem. Eng. J. 18 (2005) 127–137.
[9] M. Asadullah, M.A. Rahman, M.M. Ali, M.A. Motin, M.B. Sultan, M.R. Alam, Production of bio-oil from fixed bed pyrolysis of bagasses, Fuel 86 (2007) 2514–2520.
[10] L.C. Ferreira, P.J. Nilsen, F. Fdz-Polanco, S.I. Perez-Elvira, Biomethane potential of wheat straw: influence of particle size, water impregnation and thermal hydrolysis, Chem. Eng. J. 242 (2014) 254–259.
[11] I. Lewandowski, J.C. Clifton-Brown, J.M.O. Scurlock, W. Huisman, Miscanthus: European experience with a novel energy crop, Biomass Bioenergy 19 (2000) 209–227.
[12] W.H. Chen, B.J. Lin, Characteristics of products from the pyrolysis of oil palm fiber and its pellets in nitrogen and carbon dioxide atmospheres, Energy 94 (2016) 569–578.
[13] M.N. Islam, M.R.A. Beg, M.R. Islam, Pyrolytic oil from fixed bed pyrolysis of municipal solid waste and its characterization, Renew. Energy 30 (2005) 413–420.
[14] M.K.K. Figueiredo, G.A. Romeiro, R.N. Damasceno, Low temperature conversion (LTC) of castor seeds – a study of the oil fraction (pyrolysis oil), J. Anal. Appl. Pyrol. 86 (2009) 53–57.
[15] D.S. Ogunniyi, Castor oil: a vital industrial raw material, Bioresour. Technol. 97 (2006) 1086–1091.
[16] A.K. Jain, A. Suhane, Research approach and prospects of non edible vegetable oil as a potential resource for biolubricant – a review, Adv. Eng. Appl. Sci. 1 (2012) 23–32.
[17] N.J. Fox, G.W. Stachowiak, Vegetable oil-based lubricants – a review of oxidation, Tribol. Int. 40 (2007) 1035–1046.
[18] A. Guerci, S. Antonio, Various uses of the castor oil plant (*Ricinus communis* L.) a review, J. Ethnopharmacol. 5 (1982) 117–137.
[19] D.I. Spalding, The combustion of liquid fuels, Fuel 32 (1953) 169–185.
[20] V.M. Ivanov, P.I. Nefedov, Experimental Investigation of the Combustion Process in Nature and Emulsified Fuels, NASA TT F-258, 1965.
[21] C.H. Wang, C.K. Law, Microexplosion of fuel droplets under high pressure, Combust. Flame 59 (1985) 53–62.
[22] C.H. Wang, J.T. Chen, An experimental investigation of the burning characteristics of water-oil emulsions, Int. Commun. Heat Mass 23 (1996) 823–834.
[23] S.C.A. Lam, A. Sobiesiak, Biodiesel droplet combustion, J. Kones Powertrain Transp. 13 (2006) 267–274.
[24] I.N.G. Wardana, Combustion characteristics of jatropha oil droplet at various oil temperatures, Fuel 89 (2010) 659–664.
[25] S.S. Hou, F.M. Rizal, T.H. Lin, T.Y. Yang, H.P. Wan, Microexplosion and ignition of droplets of fuel oil/bio-oil (derived from lauan wood) blends, Fuel 113 (2013) 31–42.
[26] M. Tsue, T. Kadota, D. Segawa, H. Yamasaki, Statistical analysis on onset of microexplosion for an emulsion droplet, in: Twenty-Sixth Symposium (International) on Combustion, The Combustion Institute, 1996, pp. 1629–1635.
[27] L. Tognotti, A. Malotti, L. Petarca, S. Zanelli, Measurement of ignition temperature of coal particles using a thermogravimetric technique, Combust. Sci. Technol. 44 (1985) 15–28.
[28] J.C. Crelling, E.J. Hippo, B.A. Woerner, D.P. West Jr., Combustion characteristics of selected whole coals and macerals, Fuel 71 (1992) 151–158.
[29] X. Huang, X. Jiang, X. Han, H. Wang, Combustion characteristics of fine- and micro-pulverizes coal in the mixture of O_2/CO_2, Energy Fuels 22 (2008) 3756–3762.
[30] M. Sami, K. Annamalai, M. Wooldridge, Co-firing of coal and biomass fuel blends, Prog. Energy Combust. Sci. 27 (2001) 171–214.
[31] J.J. Lu, W.H. Chen, Investigation on the ignition and burnout temperatures of bamboo and sugarcane bagasse by thermogravimetric analysis, Appl. Energy 160 (2015) 49–57.
[32] Y. Zhang, M. Gu, B. Ma, H. Chu, Study on co-combustion characteristics of superfine coal with conventional size coal in O_2/CO_2 atmosphere, Energy Power Eng. 5 (2013) 36–40.
[33] Y. Jin, Y. Li, F. Liu, Combustion effects and emission characteristics of SO_2, CO, NOx and heavy metals during co-combustion of coal and dewatered sludge, Front. Environ. Sci. Eng. 10 (2015) 201–210.
[34] J.Y. Cheng, X.X. Sun, Determination of the devolatilization index and combustion characteristic index of pulverized coals, Power Eng. 7 (1987) 13–18.
[35] M. Fakhrur Rizal, Burning of Fuel Oil Mixed with Biofuel Derived from Lauan, Master Thesis, National Cheng-Kung University, 2012.
[36] M.J. Wornat, B.G. Porter, N.Y.C. Yang, Single droplet combustion of biomass pyrolysis oils, Energy Fuels 8 (1994) 1131–1142.
[37] R.K. Singh, K.P. Shadangi, Liquid fuel from castor seeds by pyrolysis, Fuel 90 (2011) 2538–2544.
[38] M.M. Conceição, V.J. Fernandes Jr., A.S. Araújo, M.F. Farias, I.M.G. Santos, A.G. Souza, Thermal and oxidative degradation of castor oil biodiesel, Energy Fuels 21 (2007) 1522–1527.
[39] J.W. Li, A Study of Thermal Process for Sewage Sludge Pyrolytic Oil and its Combustion Characteristics, Master Thesis, National Cheng-Kung University, 2016.